THE JOURNAL OF PHYSICAL CHEMISTRY C

Article

pubs.acs.org/JPCC

Beveled Oxide Study of the Surface Potential Modulation of Self Assembled Alkyltrichlorosilanes

Lior Kornblum,*[†,‡] Yair Paska,[‡,§] Hossam Haick,[‡,§] and Moshe Eizenberg[†,‡]

[†]Department of Materials Science & Engineering, [‡]The Russell Berrie Nanotechnology Institute, and [§]Department of Chemical Engineering, Technion − Israel Institute of Technology, Haifa 32000, Israel

Supporting Information

ABSTRACT: Despite its promise for science and application, the electrostatic origins of the surface potential modulation caused by self-assembled monolayers (SAMs) are still not fully clear. Recently the beveled oxide method has been demonstrated as a means of measuring the electrostatic effects induced by SAM, based on a series of metal-oxide-semiconductor capacitors. In this work the beveled oxide method is expanded and applied on a series of four different alkyltrichlorosilanes monolayers. It is found that hexyltrichlorosilanes produce the largest modulation among the measured molecules. The application and limitations of the method are further discussed.

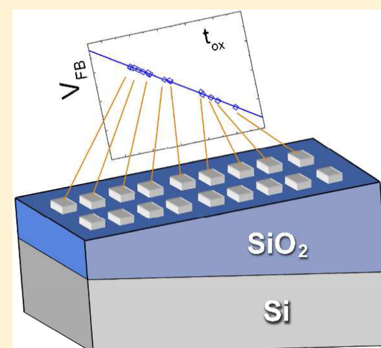

1. INTRODUCTION

Self-assembled monolayers (SAMs) offer a wide range of opportunities for science and applications. The promise of SAMs stems from their ability to use chemistry as a bridge between the molecular level and the macroscopic world. Earlier results have shown that SAMs can modify the surface and interface properties of semiconductors significantly. Important improvements have been observed by potential modulation caused by SAMs in electronics and electro-optics ranging from solar cells[1] to electronic devices[2,3] and sensors.[4−7]

A net layer of electrical dipole moments perpendicular to a surface can produce a substantial shift in surface potentials, i.e., in the work function of a metal,[8] and in the electron affinity and work function of a semiconductor.[9] To first order approximation, these changes are due to rigid shifts in the electrostatic potential across the adsorbed molecular layers. This explanation becomes less straightforward when applied to back-gated silicon-on-insulator field effect transistors (SOIFET),[10−14] a useful structure for (bio)chemical sensors as well as other (opto)electronic devices.[4] In SOIFET devices the molecules are positioned on the opposite side of the channel, namely, at the Si−air interface. If the SAM would form an ideal dipole layer, its effect on the device in such geometries would have been negligible, in contrast to the experimental observations. This alleged contradiction was discussed in detail by Natan et al.,[15] who stressed the contribution of long-range effects between molecules such as those caused by ordering and defects in the monolayer.

Alternatively, the surface potential modulation can be caused by the effect of the SAM on interface states.[16,17] Such an effect can be the creation of states in the free surface of the oxide or semiconductor that in the case of very thin (native) oxides could possibly change the density of states at the semiconductor−oxide interface. Charging of such states can explain the SOIFET behavior discussed above and account for many of the electrostatic effects caused by SAMs. Such effects have been discussed in detail in a recent work.[17] Capua et al. have systematically addressed the role of dipoles versus surface or interface states and found that in practice there is no general answer and that this question further depends on the semiconductor and its surface.[18]

The surface potential modulation is commonly studied by a Kelvin probe (KP), which is usually referred to as a contact potential difference (CPD) measurement.[9,11,19] In earlier studies, the potential modulation was estimated from the barrier heights of Schottky diodes extracted from current−voltage (I−V),[20,21] I−V temperature,[22] and capacitance−voltage (C−V)[23] measurements. In addition, internal photoemission (IPE) measurements were used for the investigation of the electronic structure of SAMs.[24] However, most of the relevant SAMs are bound to the surface of semiconductors through a thin layer of oxide, commonly the native oxide of the semiconductor.[6,20] This thin layer assists the grafting of SAMs but adds complexity to most of the above-mentioned measurements and their interpretation.

Recently, we have demonstrated an approach to study the electrostatic properties of the SAMs while avoiding the complexities associated with the thin native oxide.[25] The method is based on the application of the beveled oxide method, which is commonly used in metal oxide semiconductor

Received: August 21, 2012
Revised: December 2, 2012
Published: December 19, 2012

ACS Publications © 2012 American Chemical Society

(MOS) studies,[26−28] for the extraction of the surface potential modulation of hexyltrichlorosilane (HTS) from the effective work function (EWF) of the gate. In this method, the oxide substrate of the SAM is thicker and insulating, in contrast to Schottky-based methods, thus avoiding the complexities of a thin native oxide. This is done by the replacement of the native oxide with a controllable, high-quality thermally grown SiO_2, namely, changing the metal-semiconductor contact to an MOS capacitor. In the current work the beveled oxide method is applied on SAMs of trichlorosilanes with different alkyl chains lengths with the goal of gaining further insight on the physical origin of the surface potential modulation. To this end, a series of systematically varied chain lengths of alkyl molecules and/or functional groups (CF_3 vs CH_3) are studied and compared. In the current paper, the beveled oxide method is discussed beyond the scope of the previous work,[25] with emphasis on interpretation and the method's limitations. Solving the dilemma about the role of dipoles or surface/interface states is beyond the scope of this paper, but the application and discussion of our method provides a different route to measure the SAMs under different electrostatic conditions, which can provide new perspective on the matter.

2. EXPERIMENTAL METHODS

2.1. Beveled Oxide Substrate Preparation. The preparation of beveled oxide substrates was carried out similarly to our previous work.[25] 55 nm of SiO_2 were grown on an RCA-cleaned (100) 8″ p-Si wafer (B ∼ 2 × 10^{13} cm^{-3}) by dry thermal oxidation. The wafers were then cleaved in half and each half was gradually immersed in a dilute hydrofluoric solution in water (1:10) for ∼100 s to form a beveled structure, schematically shown in Figure 1. A back contact was formed by e-beam evaporation of 300 nm Al.

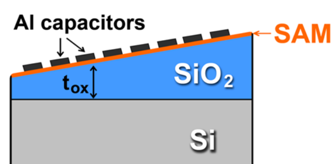

Figure 1. Schematic cross section of a SAM beveled oxide sample.

2.2. SAM deposition. The SAM deposition is based on the two-step amine-promoted reaction using a recipe that was studied in detail[29] and applied in various previous works.[6,12,17,25] Details about the molecules used here are specified in Table 1. The substrates were thoroughly cleaned and sonicated in chloroform (CF). Surface activation was done by a UV ozone cleaning system (UVOCS) followed by CF sonication, and after drying in N_2 the substrates were heated to 300 °C for 30 min. The surfaces were then exposed to trimethylamine (TMA) gas for 3 min followed by immersion for 1 h in a dilute 1.5 mM solution of the SAM molecules (specified in Table 1) in CF. The samples were rinsed and sonicated again in CF to remove molecular residues, and dried in a N_2 flow.

Table 1. Names, Abbreviations, Formulas and Chemical Purity of the Different SAM Molecules

molecule	abbreviation	formula	chemical purity (manufacturer)
propyl-trichlorosilane	C3	$SiCl_3(CH_2)_2CH_3$	98% (Sigma-Aldrich)
3,3,3-trifluoropropyl-trichlorosilane	C3F3	$SiCl_3(CH_2)_2CF_3$	97% (Sigma-Aldrich)
hexyl-trichlorosilane	C6	$SiCl_3(CH_2)_5CH_3$	97% (Sigma-Aldrich)
dodecane-trichlorosilane	C12	$SiCl_3(CH_2)_{11}CH_3$	≥95.0% (GC) (Sigma-Aldrich)

2.3. MOS Capacitors Fabrication and Measurements. MOS capacitors were formed after SAM deposition by e-beam evaporation of 40 nm of Al at a rate of 0.4 nm/s through a shadow mask with a defined contact area of 2.5 × 10^{-3} cm^2 (on average, this yields a negligible SiO_2 thickness gradient of 0.25 nm across a capacitor). Capacitance−voltage (C−V) measurements were done in a light-sealed chamber at 100 kHz using an HP4284A LCR meter. The use of low-doping wafers resulted in a high series resistance (R_S) value of 1.7 KΩ which was corrected following the measurement.[30] The area of each capacitor was measured separately using an optical microscope to account for small possible mask variations. Starting from the SAM preparation, all of the subsequent processing and measurements were performed in the same day to ensure the freshness and cleanness of the samples.

2.4. X-ray Photoelectron Spectroscopy (XPS). Some capacitors deposited on SAM were peeled-off from the substrates using an adhesive tape and the XPS spectra were collected from the underlying SiO_2. Measurements were done using a Thermo VG Scientific Sigma Probe with a monochromatic Al Kα (1486.6 eV) source and a pass energy of 20 eV. Si 2p peak fitting was done with a doublet separation of 0.61 eV, a Shirley type background, and a 13% Lorentzian−Gaussian ratio.

3. RESULTS

The flat band voltage, V_{FB},[30] is a key parameter when the beveled oxide method is used. It is an important parameter as it is easily extracted from a C−V measurement and it contains useful physical information on an MOS capacitor. The purpose of the beveled oxide method is to separate the electrostatic contributions to the V_{FB} from the EWF of the metal. As discussed elsewhere[25] it is convenient to express V_{FB} in the following manner:

$$V_{FB} = (\phi_M^{eff} + \Delta) - \phi_S - (Q_f/\varepsilon_{ox}) \times t_{ox} \quad (1)$$

where ϕ_M^{eff} is the EWF of the metal, Δ the surface potential modulation of the SAM, ϕ_s the Si work function, Q_f the Si−SiO_2 interface charge, ε_{ox} the SiO_2 permittivity, and t_{ox} the SiO_2 thickness extracted from the oxide capacitance in accumulation.[30] The basic principle of the surface potential modulation measurement by this method is to plot V_{FB} versus t_{ox}, and subtract the intercepts of a SAM sample from a "bare" reference sample. This yields exactly the value of Δ.

Deposition of metals by e-beam evaporation is well-known to induce a high density of electrically active defects in an MOS device.[31,32] These defects are usually significantly reduced after annealing at 400−600 °C, which is not performed on organic monolayers for obvious reasons. The most important electrical defects are manifested by Si−SiO_2 interface charges (Q_f) and SiO_2−Si interface states. Bulk SiO_2 charges would add a cubic term to eq 1 (refs 28 and 33) and would be observed as a nonlinearity in V_{FB} versus t_{ox} dependence. Interface charges are accounted for straightforwardly in eq 1. By contrast, SiO_2−Si

interface states are not included in eq 1 as their contribution to the V_{FB} is complex and its quantification requires rigorous modeling.[30] However, if the Al contacts of the bare reference and the SAM sample(s) are deposited simultaneously, then the contribution of the interface states would be identical. For this reason, the EWF determined from each sample should not be considered as an absolute value but only as a reference for the extraction of Δ. As will be shown in this work, the electrical defects can vary significantly between different depositions, even when performed under identical conditions, stressing the importance of a bare reference sample in every sample set.

In addition to the deposition damage, slightly different slopes ($-Q_f/\varepsilon_{ox}$) are obtained for samples that underwent the same deposition. This difference is attributed to trace chemical residues, some of which may cause changes of the charges of the SiO_2.

Examples of some of the C−V curves of bare, C6, and C12 SAM samples are presented in Figure 2. A difference in the shape and slope of a C−V curve is indicative of different quantity and energy distribution of Si−SiO_2 interface states. To verify that such a change does not affect the V_{FB} extraction, each curve in Figure 2 was horizontally shifted to superimpose the adjacent bare curve. This demonstrates that the SAMs do not change the shape of the C−V curves, only their horizontal position. Unlike the common substrate for SAMs, native oxides, in the beveled oxide method the Si−SiO_2 interface is separated from the SiO_2−SAM interface by many nanometers of SiO_2 (15−55 nm in the present work). This feature offers a different electrostatic view of the surface potential modulation with respect to some of the other methods. The arrows in Figure 2 further highlight the increase of t_{ox} (with the capacitance decrease) in parallel with a shift of V_{FB}, in accordance with eq 1.

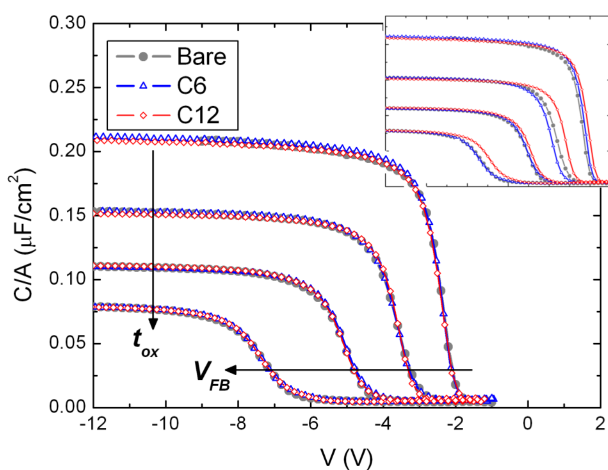

Figure 2. Capacitance−voltage curves of bare, C6, and C12 samples with t_{ox} = 16, 23, 31, and 44 nm. For each thickness the curve is superimposed on that of the bare sample, demonstrating that the Si−SiO_2 interface states density is not affected by the SAM. Inset shows the unshifted data.

The metal deposition process in this work was done in two runs: the first on C6, C12, and bare substrates ("bare1") and the second on C3, C3F3, and bare substrates ("bare2"). Figure 3 shows V_{FB} versus t_{ox} plots for the two bare samples, showing a clear difference in both the slope and the intercept. Both differences are caused by the difference in deposition-induced electrical defects, and demonstrate the importance of using a reference sample in every set of samples as discussed before.

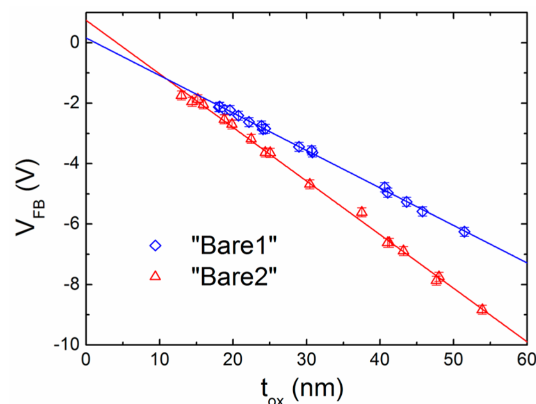

Figure 3. V_{FB}−t_{ox} plot comparing the bare reference samples done in two separate Al depositions. The vertical error bars have the same size as the data points.

Given the differences demonstrated in Figure 3, a different way of displaying the V_{FB}−t_{ox} plot is hereby proposed: the vertical axis of the plot is transformed to represent the difference between the V_{FB} of a SAM sample from the linear fit of its bare reference curve. This representation allows displaying the data obtained from separate sample sets, while each is measured with respect to its own reference. This relative representation is used to display the data measured for the four different alkyltrichlorosilanes (Table 1) in Figure 4a. In addition, data from the previous work[25] is superimposed on Figure 4 under the name C6 (APL).

The surface potential modulation of the different SAMs, extracted from the intercepts of Figure 4a, is summarized in

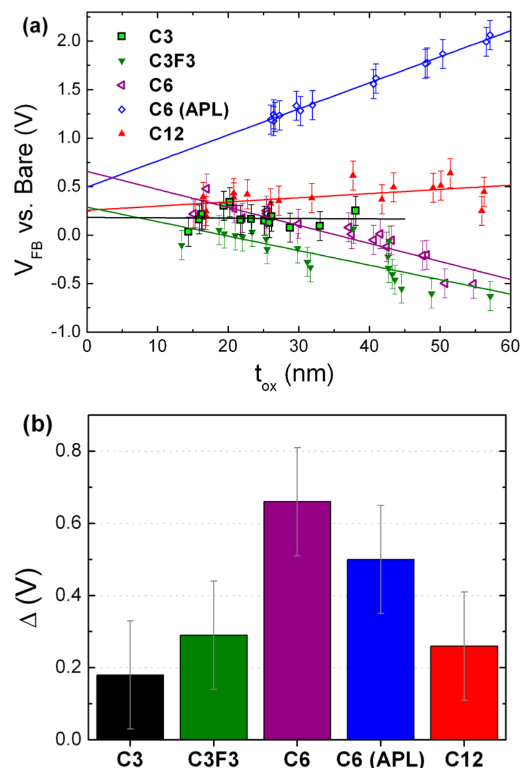

Figure 4. (a) Relative V_{FB}−t_{ox} plot for C3, C3F3, C6, and C12 SAM. (b) A summary of the values of the surface potential modulation (Δ) of the different SAM.

Figure 4b. The results show that C6 is the most efficient SAM in terms of surface potential modulation, among the molecules studied here. The C6 results are in agreement with the previous work, within the range of the experimental error. The error in V_{FB} and in Δ is estimated as ± 0.15 V, which represents the maximal possible difference in the shape of a C−V curve between different samples of the same set, and the possible change in the intercept should one data point be removed. The maximal error values from all of the data are used for all of the samples, meaning that in practice some errors may be smaller. In contrast, the C3 sample has the lowest measured surface potential modulation, which is just barely larger than the experimental error.

In order to obtain structural information about the SAMs, XPS spectra were collected from the exposed substrates after peeling off ("delaminating") the capacitors (Figure 5).

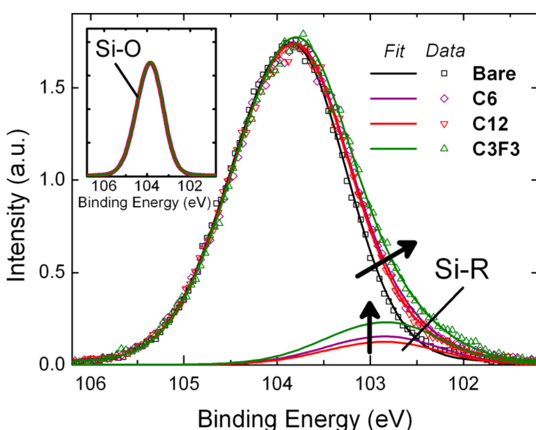

Figure 5. Si 2p XPS spectra of the bare sample and delaminated C6, C12, and C3F3 samples. The symbols represent data points and the solid lines represent the fitted spectra and the Si−R peaks. The (overlapping) Si−O components are shown separately in the inset for clarity. The arrows represent an increasing (relative) Si−R bonding.

Acquiring the XPS signal from the substrate underneath the capacitors is important because the data is collected from SAMs that underwent metal deposition, thus accounting for possible deposition damage to the molecules. Al deposited directly on SiO_2, namely, the bare sample, is strongly bound to the SiO_2 and cannot be peeled off. Therefore the bare spectrum was collected from the area between capacitors. In contrast, capacitors deposited on SAM are easily peeled off. However, peeling off the C3 SAM was not possible. This result agrees with the small surface potential modulation value obtained for the C3 sample (Figure 4b). It is therefore concluded that the C3 molecules are either severely damaged during the metal deposition or they are initially assembled with a low surface density.

In the bare sample, the Si 2p spectrum (Figure 5) was fitted well with this single Si−O peak. The spectra of the SAMs samples were fitted with two components. The major peak, at the higher binding energy (BE) is related to Si−O bonding in SiO_2 and was aligned similarly to ref 25. In the SAM samples, the Si−O peaks were fitted to exactly match the line shape of the Si−O bonding of the bare sample (having a full width at half-maximum, FWHM of 1.25 eV). The inset of Figure 5 shows the exact overlap of the Si−O peaks (only) of the three SAM samples, displayed separately from the main spectra for clarity. Next, a peak representing Si-organics bonding (denoted as Si-R) was fitted to the SAM spectra in the following manner: the peak position was constrained to be 1 eV lower than the Si−O,[25] and the FWHM was constrained to be 1.25 eV (identical to the Si−O peak), with the Si−O peaks of the SAM samples constrained to overlap. This analysis allows a qualitative correlation between the ratio of the Si-R/Si−O peaks and N, the surface density of the silane groups of the SAM molecules. It should be noted that despite this systematic treatment, the small Si-R contribution to the spectra makes the analysis sensitive to small changes in the fitting parameters. However, even if the fitting is completely ignored; the farther the right "shoulder" of the spectrum is from the bare sample, the higher is the surface density of the silane groups, as highlighted by the slanted arrow in Figure 5.

4. DISCUSSION

When considering the dipole picture of the surface potential modulation, the Helmholtz equation can be used[29] to estimate the potential modulation from the sum of the molecular dipoles:

$$\Delta = \frac{N\mu \cos \theta}{\varepsilon\varepsilon_0} \quad (2)$$

where μ is the dipole moment of the molecule, θ the molecular tilt angle, ε the relative dielectric constant of the SAM, and ε_0 the vacuum permittivity.

When comparing the surface potential modulation of C6 and C12, a qualitative agreement is observed between the lower N, estimated from the Si−R component (Figure 5), and the lower Δ for C12 (Figure 4b). This agreement is consistent with eq 2 in the dipole picture and would also agree with a lower density in the surface states picture. It should be noted that the relative difference in N between C6 and C12 is smaller than the difference in Δ. In the frame of the dipole picture this can be attributed to another component of eq 2, namely the tilt angle. The lower density of the C12 is rather surprising, as it was found that for longer alkyl chains, the order and surface coverage of the molecules increased, particularly when the alkyl chains were longer than eight carbons.[34,35] Further information about the structure of the SAM layers is needed to explain the lower C12 density.

The C3F3 SAM shows a much higher N, ~2 times higher compared to C6, but its potential modulation is smaller than that of C6 and close to C12. This is attributed to the high electron affinity of the CF_3 tail group that reduces the surface potential modulation caused by the otherwise identical parts of the molecule.

In a study of *n*-alkyldimethylchlorosilanes, it was found that for C3 alkyl groups the chain length is shorter by ~18% than the average intermolecular distance, whereas for C8 (octyldimethylchlorosilane) the chain is longer than the average intermolecular distance.[36] It is expected that for the trichlorosilanes the intermolecular distance would be somewhat smaller. Therefore, the short alkyl chains of C3F3 may cause the molecules to arrange more horizontally, which may be further promoted by the negative tail groups. In the dipole picture, this means a further decrease in Δ by increasing θ [eq 2].

It is stressed that the discussion on the molecular arrangement and structure of the various molecules requires a detailed analysis of the structure of the SAM, such as by Fourier

transform infrared (FTIR) spectroscopy[37,38] prior to further modeling, which is beyond the scope of this work.

5. CONCLUSIONS

Following the detailed analysis of the results of this work, several lessons and limitations of the beveled oxide method are highlighted. Concerns regarding damage to the SAM caused by the deposited metal atoms can be reduced by employing indirect deposition methods using backfilling of the chamber with an inert gas (e.g., ref 22). In addition to this point, a complementary analysis of the SAM structure and chemistry (i.e., by FTIR) is required in order to get a conclusive picture of the molecular potential modulation mechanism. With respect to the beveled oxide method, the measurements in this work feature more noise with respect to the previous work.[25] This is attributed to the relatively low substrate doping level used here ($\sim 2 \times 10^{13}$ cm^{-3}) compared to $\sim 3 \times 10^{15}$ cm^{-3} used in the previous work, which can affect the accuracy of the C−V measurements. Higher substrate doping levels are therefore suggested for future work.

In summary, application of the beveled oxide method in the task of probing the SAM electrostatics provides an opportunity for acquiring new data on an old problem. Combined with a complementary structural−molecular analysis, this application can provide a powerful tool for the understanding of the electrostatics hidden at SAM−SiO_2 interfaces.

■ ASSOCIATED CONTENT

Ⓢ Supporting Information

Entire raw data used for the drawing of Figure 4a. This material is available free of charge via the Internet at http://pubs.acs.org.

■ AUTHOR INFORMATION

Corresponding Author

*E-mail: liorkorn@gmail.com. Phone: +972-4829-5798. Fax: +972-4829-5677.

Notes

The authors declare no competing financial interest.

■ ACKNOWLEDGMENTS

This work was funded by the ALPHA consortium of the Israeli Ministry of Industry, Trade and Labor. The authors thank Dr. Reuven Brener for XPS measurements and fruitful discussions and Yechiel Mozes for valuable technical assistance.

■ REFERENCES

(1) Rühle, S.; Greenshtein, M.; Chen, S. G.; Merson, A.; Pizem, H.; Sukenik, C. S.; Cahen, D.; Zaban, A. *J. Phys. Chem. B* **2005**, *109*, 18907−18913.
(2) Chung, Y.; Verploegen, E.; Vailionis, A.; Sun, Y.; Nishi, Y.; Murmann, B.; Bao, Z. *Nano Lett.* **2011**, *11*, 1161−1165.
(3) Pernstich, K. P.; Haas, S.; Oberhoff, D.; Goldmann, C.; Gundlach, D. J.; Batlogg, B.; Rashid, A. N.; Schitter, G. *J. Appl. Phys.* **2004**, *96*, 6431−6438.
(4) Cahen, D.; Naaman, R.; Vager, Z. *Adv. Func. Mater.* **2005**, *15*, 1571−1578.
(5) Goykhman, I.; Korbakov, N.; Bartic, C.; Borghs, G.; Spira, M. E.; Shappir, J.; Yitzchaik, S. *J. Am. Chem. Soc.* **2009**, *131*, 4788−4794.
(6) Paska, Y.; Stelzner, T.; Assad, O.; Tisch, U.; Christiansen, S.; Haick, H. *ACS Nano* **2011**, *6*, 335−345.
(7) Paska, Y.; Stelzner, T.; Christiansen, S.; Haick, H. *ACS Nano* **2011**, *5*, 5620−5626.
(8) Gozlan, N.; Tisch, U.; Haick, H. *J. Phys. Chem. C* **2008**, *112*, 12988−12992.
(9) Peor, N.; Sfez, R.; Yitzchaik, S. *J. Am. Chem. Soc.* **2008**, *130*, 4158−4165.
(10) He, T.; He, J.; Lu, M.; Chen, B.; Pang, H.; Reus, W. F.; Nolte, W. M.; Nackashi, D. P.; Franzon, P. D.; Tour, J. M. *J. Am. Chem. Soc.* **2006**, *128*, 14537−14541.
(11) Shaya, O.; Shaked, M.; Doron, A.; Cohen, A.; Levy, I.; Rosenwaks, Y. *Appl. Phys. Lett.* **2008**, *93*, 043509.
(12) Paska, Y.; Haick, H. *Appl. Phys. Lett.* **2009**, *95*, 233103.
(13) Shaya, O.; Shaked, M.; Usherenko, Y.; Halpern, E.; Shalev, G.; Doron, A.; Levy, I.; Rosenwaks, Y. *J. Phys. Chem. C* **2009**, *113*, 6163−6168.
(14) Shaya, O.; Einati, H.; Fishelson, N.; Shacham-Diamand, Y.; Rosenwaks, Y. *Appl. Phys. Lett.* **2010**, *97*, 053501.
(15) Natan, A.; Kronik, L.; Haick, H.; Tung, R. T. *Adv. Mater.* **2007**, *19*, 4103−4117.
(16) Bashouti, M. Y.; Tung, R. T.; Haick, H. *Small* **2009**, *5*, 2761−2769.
(17) Paska, Y.; Haick, H. *ACS Appl. Mater. Interfaces* **2012**, *4*, 2604−2617.
(18) Capua, E.; Natan, A.; Kronik, L.; Naaman, R. *ACS Appl. Mater. Interfaces* **2009**, *1*, 2679−2683.
(19) Gozlan, N.; Haick, H. *J. Phys. Chem. C* **2008**, *112*, 12599−12601.
(20) Vilan, A.; Shanzer, A.; Cahen, D. *Nature* **2000**, *404*, 166−168.
(21) Selzer, Y.; Cahen, D. *Adv. Mater.* **2001**, *13*, 508−511.
(22) Haick, H.; Ambrico, M.; Ligonzo, T.; Tung, R. T.; Cahen, D. *J. Am. Chem. Soc.* **2006**, *128*, 6854−6869.
(23) Scott, A.; Risko, C.; Valley, N.; Ratner, M. A.; Janes, D. B. *J. Appl. Phys.* **2010**, *107*, 024505.
(24) Vuillaume, D.; Boulas, C.; Collet, J.; Allan, G.; Delerue, C. *Phys. Rev. B* **1998**, *58*, 16491−16498.
(25) Kornblum, L.; Paska, Y.; Rothschild, J. A.; Haick, H.; Eizenberg, M. *Appl. Phys. Lett.* **2011**, *99*, 233508.
(26) Adelmann, C.; Meersschaut, J.; Ragnarsson, L. A.; Conard, T.; Franquet, A.; Sengoku, N.; Okuno, Y.; Favia, P.; Bender, H.; Zhao, C.; et al. *J. Appl. Phys.* **2009**, *105*, 053516.
(27) Rothschild, J. A.; Eizenberg, M. *Appl. Phys. Lett.* **2009**, *94*, 081905.
(28) Kornblum, L.; Rothschild, J.; Kauffmann, Y.; Brener, R.; Eizenberg, M. *Phys. Rev. B* **2011**, *84*, 155317.
(29) Paska, Y.; Haick, H. *J. Phys. Chem. C* **2009**, *113*, 1993−1997.
(30) Nicollian, E. H.; Brews, J. R. *MOS (metal oxide semiconductor) physics and technology*; Wiley: New York, 1982.
(31) Snow, E. H.; Grove, A. S.; Fitzgerald, D. J. *IEEE Proc.* **1967**, *55*, 1168−1185.
(32) Ning, T. H. *J. Appl. Phys.* **1978**, *49*, 4077−4082.
(33) Jha, R.; Gurganos, J.; Kim, Y. H.; Choi, R.; Lee, J.; Misra, V. *IEEE Elect. Dev. Lett.* **2004**, *25*, 420−423.
(34) Ohtake, T.; Mino, N.; Ogawa, K. *Langmuir* **1992**, *8*, 2081−2083.
(35) Turgman-Cohen, S.; Fischer, D. A.; Kilpatrick, P. K.; Genzer, J. *ACS Appl. Mater. Interfaces* **2009**, *1*, 1347−1357.
(36) Cheng, W.; McCown, M. *J. Chromatogr. A* **1985**, *318*, 173−185.
(37) Maoz, R.; Sagiv, J.; Degenhardt, D.; Möhwald, H.; Quint, P. *Supramol. Sci.* **1995**, *1*, 9−24.
(38) Baptiste, A.; Gibaud, A.; Bardeau, J. F.; Wen, K.; Maoz, R.; Sagiv, J.; Ocko, B. M. *Langmuir* **2002**, *10*, 3916−3922.